Stability-Oriented Design of MoO_3/TAPC Hybrid Bilayer Hole Transport Layer for Scalable Organic Solar Cells

*Ji Youn Kim, Ye Chan Kim, and Doo Kyung Moon**

NanoandInformation Materials (NIMs) Laboratory, Department of Chemical Engineering, Konkuk University, 120, Neungdong-ro, Gwawngjin-gu, Seoul 05029, Republic of Korea

Experimental section

1.1 **Materials**

ITO glass (sheet resistance 15 Ω/square) were purchased from AMG (Republic of Korea). Zinc acetate dehydrate (ZAD), ethanolamine (EA), and 2-methoxyethanol (2ME) for precursors of sol−gel ZnO were purchased from Sigma-Aldrich (USA). The donor and acceptor materials including PM6, L8-BO, and PDINN were purchased from Derthon (China). Solvents including chloroform (CF, ≥99%), methanol (MeOH, ≥99.8%), Diiodomethane (DIM, 99%), and 1,8-diiodooctane (DIO, 98%) were purchased from Sigma-Aldrich (USA). Molybdenum(VI) oxide (MoO_3) was purchased from Thermo Fisher Scientific (Alfa Aesar, USA). TAPC was purchased from Luminescence Technology Corp. (Taiwan). Poly(3,4-ethylenedioxythiophene):poly(styrene sulfonate) (PEDOT:PSS) (Clevious P VP AI 4083) were obtained from Heraeus (Germany).

1.2 **Experiment**

1.2.1 Preparation of ZnO sol-gel Solution

ZAD (100 mg) was dissolved into 1 mL of 2ME and 27.6 μL of EA at room temperature in air and reacted until the appearance of gels.

1.2.2 Preparation of TAPC solutions

TAPC solutions with concentrations ranging from 0.5 to 20 mg mL^{-1} were prepared by dispersed TAPC in MeOH. After optimization by using various concentration, a concentration of 0.5 mg mL^{-1}, was selected for application to OSCs. The solutions were then treated with sonication for 10 min prior to use.

1.2.3 Preparation of active layer

The blend of PM6 and L8-BO with a weight ratio (wt. ratio) of 1:1.2 was dissolved in CF containing 0.25 vol% DIO at a total concentration of 15.4 mg mL^{-1}. Notably, the blend solution preheated at 50 °C before processing.

1.2.4 Device Fabrication

Unit cell device fabrication: The OSCs were fabricated with an inverted structure of ITO/ZnO/active layer/HTLs/Ag. Patterned ITO-coated glass substrates were sequentially cleaned by ultrasonication in a detergent solution (Alconox Inc.), isopropanol, and deionized water for 10 min each. The ITO substrates were then dried with a nitrogen gun and thermally treated at 100 °C for 10 min to ensure complete removal of residual moisture. Subsequently, they were subjected to UV–ozone (UVO) cleaning using a UVO cleaner (Ahtech LTS) for 20 min. The ZnO sol-gel solution was spin-coated onto the cleaned ITO substrates at 2500 rpm for 30 s under ambient conditions, which resulted in a 20 nm thick layer, followed by thermal annealing at 150 °C for 30 min. Afterward, the blended active layer solution was spin-coated at 3000 rpm for 30 s, resulting in a 150 nm thick film, and then thermally annealed at 100 °C for 10 min. For the single-layer MoO_3 device, a 2.5 nm thick MoO_3 layer was thermally deposited at a rate of 0.3 Å s^{-1}. For the MoO_3/TAPC hybrid HTL device, a TAPC layer was spin-coated at 3000 rpm for 30 s, followed by thermal deposition of a 2.5 nm MoO_3 layer at the same rate.

Finally, a 100 nm Ag electrode was deposited at a rate of 1.0 Å s^{-1} under vacuum conditions. The active area of the fabricated devices was defined by a shadow mask and measured as 0.04 cm^2.

Module-device fabrication**:** The fabrication procedure of the module devices was largely identical to that of the unit cells. The P1 pattern on the ITO substrate was pre-designed according to the specified layout and purchased from AMG Corporation. After substrate cleaning, the ETL was coated following the same procedure used in the unit cell fabrication. The P2a patterning was performed prior to annealing of the ZnO sol-gel layer using a methanol-soaked cotton swab. Subsequently, the photoactive layer and the TAPC layer were sequentially coated using the same methods as in the unit cell process, followed by P2b patterning using a methanol-soaked cotton swab. Finally, P3 patterning was completed by thermally evaporating a 100 nm Ag layer through a custom-designed shadow mask under high vacuum conditions (below 10^{-7} Torr).

1.3 Instruments and Characterizations

Current density–voltage (*J*–*V*) characteristics were measured using a Keithley 2400 source meter. The photocurrent was measured under AM 1.5 G illumination under at 100 mW cm^{-2} using a Oriel solar simulator. The EQE spectrum was measured by using Polaronix K3100 IPCE (Mc science, Korea). The internal quantum efficiency (IQE) spectra were determined using the measured EQE and reflectance (*R*) spectra according to the relation: IQE = EQE / (1−R). The chemical composition and electronic states of the films were characterized by X-ray photoelectron spectroscopy (XPS) using a K-Alpha spectrometer (Thermo Scientific) with using a monochromatic Al-Kα X-ray source (NFEC-2019-01-248114). The thicknesses were measured using a F20 UV reflectometer (Filmetrics, Inc., USA). The photoluminescence (PL) spectra were analyzed using a Perkin Elmer LS-55 spectrofluorometer. UV-Vis spectra were tested by Agilent 8453. Atomic force microscopy (AFM) measurements were carried out using a PSIA XE-100 (Park Systems) in non-contact mode over a scan area of 5 μm × 5 μm to obtain surface height and phase images. Contact angle measurements were performed using a Theta Flex (Attension) system. A constant droplet volume of 3 μL of deionized water and DIM was deposited onto substrate prepared by spin-coating under ambient conditions. Surface energy was calculated using the Wu model.[1] The carrier mobilities of single-layer MoO_3 (control) device and MoO_3/TAPC hybrid HTL device were investigated by the space charge limited current (SCLC) method. As in previous reports,[2] the hole mobility of the control films was measured with hole mobility device structure of ITO/PEDOT:PSS/active layer/MoO_3/Ag (100 nm), while the TAPC-based films was with the device structure of ITO/PEDOT:PSS/active layer/TAPC/MoO_3/Ag (100 nm).:

$$J = \frac{9}{8}\varepsilon_0\varepsilon_r\mu\left(\frac{V^2}{L^3}\right) \tag{S1}$$

where J represents the current density, ε_0 is the permittivity of free space (8.85×10^{-12} $C\cdot V^{-1}\cdot m^{-1}$), ε_r is the relative permittivity, μ is the carrier mobility, V is the internal potential in the device, and L is the thickness of the HTLs (≈ 30 nm). Electrochemical impedance spectroscopy (EIS) measurements were performed using a CompactStat2.h potentiostat (IVIUM Technologies) to evaluate the interfacial resistance characteristics of the fabricated OSCs. The measurements were conducted under dark conditions over a frequency range of 1 Hz to 4 MHz.

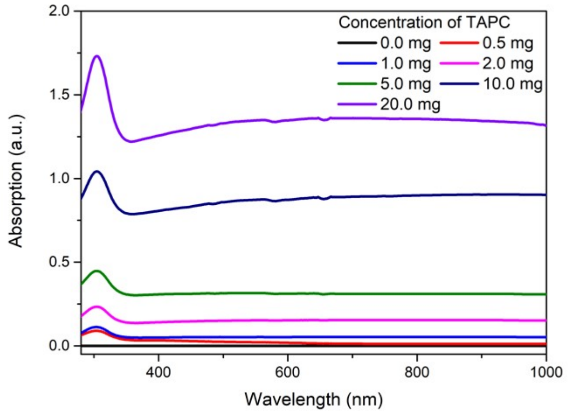

Figure S1. UV–Vis absorption spectra of TAPC solutions in methanol with concentrations ranging from 0.5 to 20 mg/mL, prepared by ultrasonication.

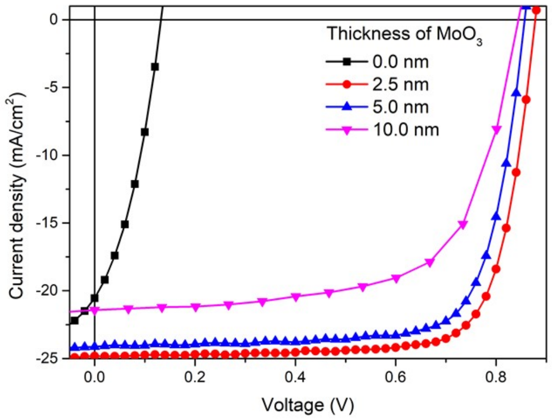

Figure S2. Current density–voltage (*J*–*V*) characteristics of PM6:L8-BO-based OSCs varying MoO_3 thicknesses (0, 2.5, 5, and 10 nm) under AM 1.5G illumination (100 mW cm^{-2}) for optimization.

Table S1. Photovoltaic parameters of PM6:L8-BO-based OSCs with various MoO_3 thicknesses with 0.5mgmL^{-1} of TAPC under AM 1.5G illumination (100 mW cm^{-2}) for optimization.

Thickness of MoO_3	J_{SC} [mA cm^{-2}]	V_{OC} [V]	FF [%]	PCE [%]
0.0 nm	20.55	0.132	35.76	0.97 (0.72 ± 0.17)
2.5 nm	24.33	0.880	76.58	16.39 (16.34 ± 0.15)
5.0 nm	23.53	0.873	76.54	15.71 (15.46 ± 0.17)
10.0 nm	21.42	0.844	66.03	11.94 (11.86 ± 0.18)

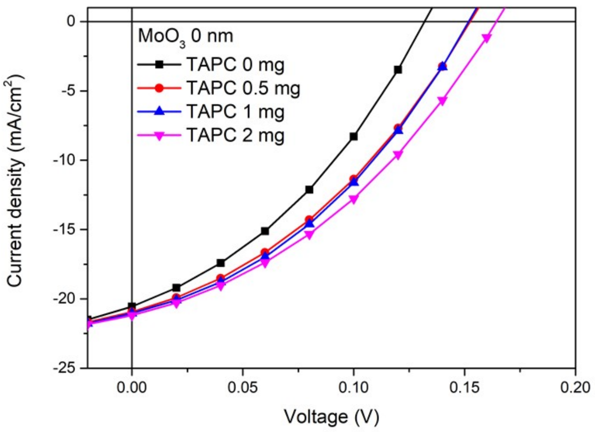

Figure S3. *J–V* characteristics with varying TAPC concentrations (0, 0.5, 1.0, and 2.0 mg/mL) at fixed MoO$_3$ thickness of 0 nm.

Table S2. Photovoltaic parameters of OSCs with different TAPC concentrations at a fixed MoO$_3$ thickness of 0 nm.

TAPC concentration [mgmL^{-1}]	J_{SC} [mA cm^{-2}]	V_{OC} [V]	FF [%]	PCE [%]
0.0	20.55	0.132	35.76	0.97 (0.723 ± 0.17)
0.5	20.94	0.153	35.84	1.14 (0.863 ± 0.23)
1.0	21.03	0.152	36.59	1.17 (0.913 ± 0.16)
2.0	21.18	0.164	36.68	1.28 (1.12 ± 0.11)

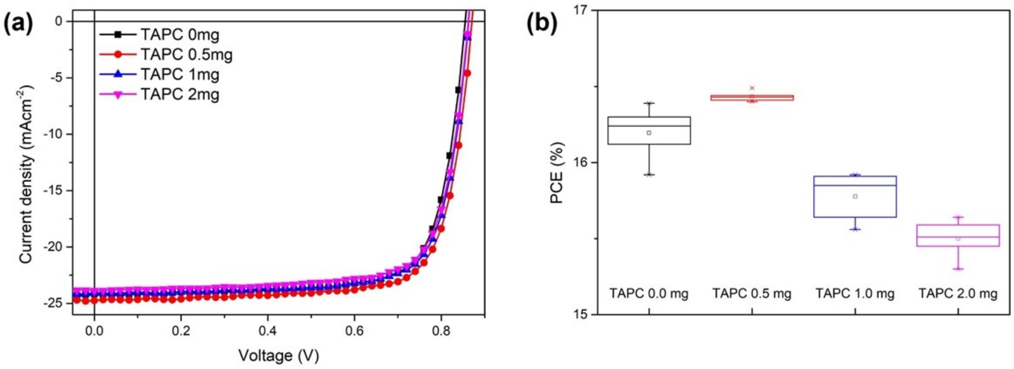

Figure S4. (a) Current density–voltage (*J*–*V*) characteristics and (b) the PCE distribution of devices according to TAPC concentrations optimization.

Table S3. Photovoltaic parameters of OSCs with different TAPC concentrations at a fixed MoO_3 thickness of 2.5 nm.

TAPC concentration [mgmL^{-1}]	Thickness [nm]	J_{SC} [mA cm^{-2}]	V_{OC} [V]	FF [%]	PCE [%]
0.0	0.00	24.33	0.880	76.58	16.39 (16.34 ± 0.15)
0.5	28.50	24.48	0.882	76.35	16.49 (16.44 ± 0.03)
1.0	29.30	24.09	0.863	76.63	15.92 (15.78 ± 0.15)
2.0	36.90	23.87	0.862	75.99	15.64 (15.50 ± 0.12)

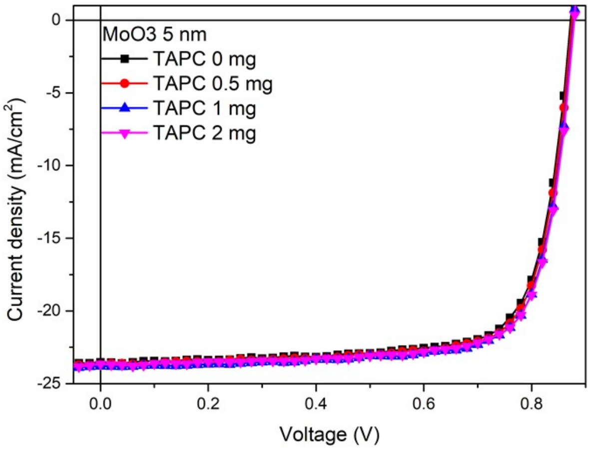

Figure S5. *J*–*V* characteristics with varying TAPC concentrations (0, 0.5, 1.0, and 2.0 mg/mL) at fixed MoO_3 thickness of 5 nm.

Table S4. Photovoltaic parameters of OSCs with different TAPC concentrations at a fixed MoO_3 thickness of 5 nm.

TAPC concentration [mgmL^{-1}]	J_{SC} [mA cm^{-2}]	V_{OC} [V]	FF [%]	PCE [%]
0.0	23.53	0.873	76.54	15.71 (15.46 ± 0.17)
0.5	23.69	0.875	76.79	15.91 (15.83 ± 0.10)
1.0	23.80	0.878	76.86	16.06 (15.98 ± 0.05)
2.0	23.67	0.879	77.31	16.08 (16.07 ± 0.02)

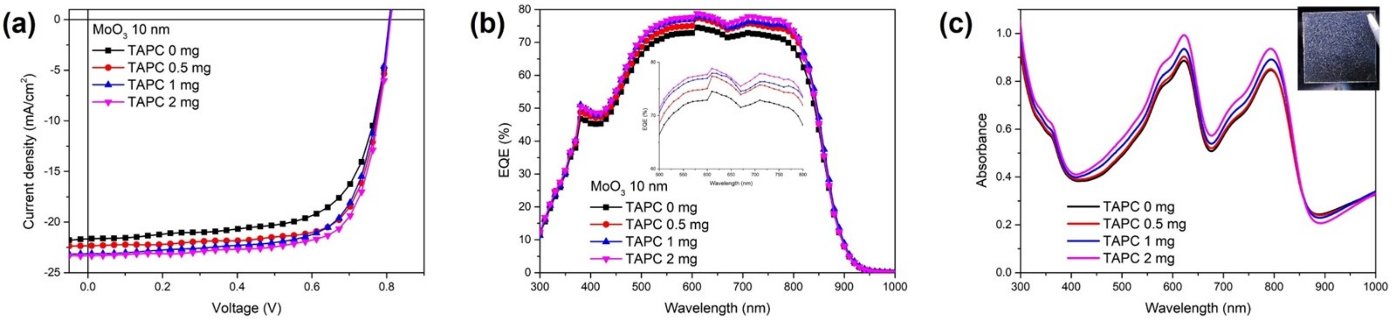

Figure S6. (a) *J–V* characteristics and (b) EQE with varying TAPC concentrations (0, 0.5, 1.0, and 2.0 mg/mL) at fixed MoO_3 thickness of 10 nm. (c) UV-Vis absorption spectra of the active layer films with structure of ITO/active layer/MoO_3(black line) ITO/active layer/TAPC/MoO_3(red line). The inset photograph shows the visual appearance of the MoO3/TAPC hybrid HTL film.

Table S5. Photovoltaic parameters of OSCs with different TAPC concentrations at a fixed MoO_3 thickness of 10 nm.

TAPC concentration [mgmL^{-1}]	J_{SC} [mA cm^{-2}]	J_{Cal} [mA cm^{-2}]	V_{OC} [V]	FF [%]	PCE [%]
0.0	21.66	20.99	0.810	67.83	11.91 (11.64 ± 0.26)
0.5	22.34	21.77	0.831	73.66	13.68 (13.59 ± 0.07)
1.0	23.13	22.22	0.804	70.64	13.14 (13.03 ± 0.11)
2.0	23.33	22.34	0.822	73.47	14.09 (13.92 ± 0.12)

[a] J_{cal} values were obtained from the EQE curves.

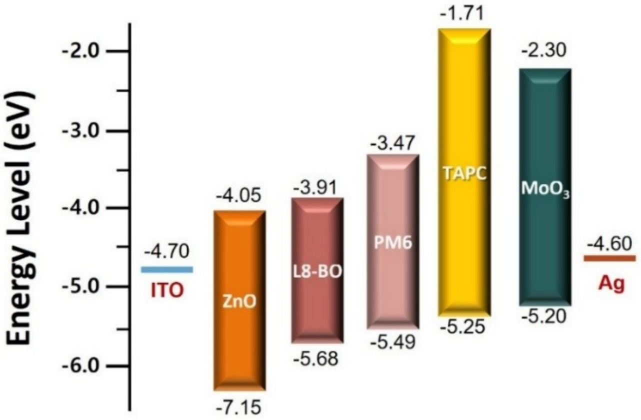

Figure S7 Schematic energy level diagram of the inverted OSC device structure: ITO/ZnO/PM6:L8-BO/TAPC/MoO_3/Ag.

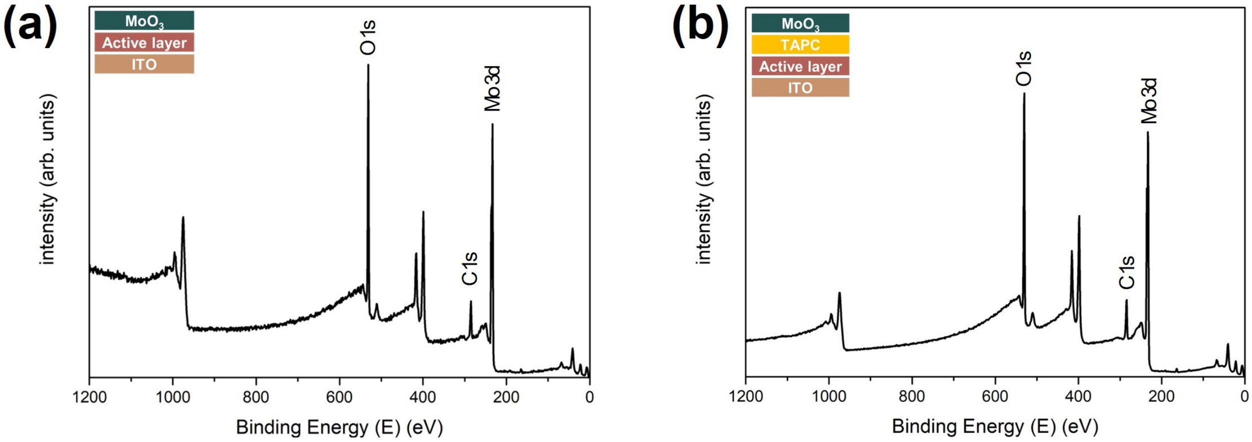

Figure S8 XPS survey scan of ITO/BHJ/MoO_3 and ITO/BHJ/TAPC/MoO_3 films.

Table S6. Photovoltaic parameters of the optimized single-layer MoO3 device and MoO_3/TAPC hybrid HTL

	J_{SC} [mA cm^{-2}]	V_{OC} [V]	FF [%]	PCE [%]
Single-layer MoO_3 device	21.64	0.780	62.12	10.48 (10.42 ± 0.06)
MoO_3/TAPC hybrid HTL device	21.78	0.794	64.44	11.15 (11.12 ± 0.03)

OSCs with 1cm^2.

Reference

1 Y. C. Kim, S. J. Jeon, N. G. Yang, J. Y. Kim, Y. W. Han and D. K. Moon, *ACS Appl Mater Interfaces*, 2025, **17**, 6626–6638.

2 W. Wang, Z. Lin, X. Li, C. Zhang, T. Yang and Y. Liang, *ACS Appl Mater Interfaces*, 2022, **14**, 18736–18743.